STEM CELLS
TRANSLATIONAL MEDICINE®

Autologous Bone Marrow Mesenchymal Stem Cells Improve the Quality and Stability of Vascularized Flap Surgery of Irradiated Skin in Pigs

CHRISTINE LINARD [iD],[a]* MICHEL BRACHET,[b]* CARINE STRUP-PERROT,[a] BRUNO L'HOMME,[a] ELODIE BUSSON,[c] CLAIRE SQUIBAN,[a] VALERIE HOLLER,[a] MICHEL BONNEAU,[d] JEAN-JACQUES LATAILLADE,[c] ERIC BEY,[b] MARC BENDERITTER[a]

Key Words. Mesenchymal stromal cell • Skin • Pig • Irradiation

[a]Institute of Radiological Protection and Nuclear Safety, Fontenay-aux-Roses, France; [b]Department of Plastic Surgery, Military Hospital of Percy, Clamart, France; [c]Research and Cell Therapy Department, Military Blood Transfusion Center, Percy Military Hospital, Clamart, France; [d]Centre of Research in Interventional Imaging, National Institut of Agronomic Research, Jouy-en-Josas, France

Correspondence: Christine Linard, Ph.D., Institut de Radioprotection et de Sûreté Nucléaire, B.P. n°17, Fontenay-aux-Roses F-92262, France. Telephone: +33 1 58 35 91 86; e-mail: christine.linard@irsn.fr

*Contributed equally.

ABSTRACT

Cutaneous radiation syndrome has severe long-term health consequences. Because it causes an unpredictable course of inflammatory waves, conventional surgical treatment is ineffective and often leads to a fibronecrotic process. Data about the long-term stability of healed wounds, with neither inflammation nor resumption of fibrosis, are lacking. In this study, we investigated the effect of injections of local autologous bone marrow-derived mesenchymal stromal cells (BM-MSCs), combined with plastic surgery for skin necrosis, in a large-animal model. Three months after irradiation overexposure to the rump, minipigs were divided into three groups: one group treated by simple excision of the necrotic tissue, the second by vascularized-flap surgery, and the third by vascularized-flap surgery and local autologous BM-MSC injections. Three additional injections of the BM-MSCs were performed weekly for 3 weeks. The quality of cutaneous wound healing was examined 1 year post-treatment. The necrotic tissue excision induced a pathologic scar characterized by myofibroblasts, excessive collagen-1 deposits, and inadequate vascular density. The vascularized-flap surgery alone was accompanied by inadequate production of extracellular matrix (ECM) proteins (decorin, fibronectin); the low col1/col3 ratio, associated with persistent inflammatory nodules, and the loss of vascularization both attested to continued immaturity of the ECM. BM-MSC therapy combined with vascularized-flap surgery provided mature wound healing characterized by a col1/col3 ratio and decorin and fibronectin expression that were all similar to that of nonirradiated skin, with no inflammation, and vascular stability. In this preclinical model, vascularized flap surgery successfully and lastingly remodeled irradiated skin only when combined with BM-MSC therapy. STEM CELLS TRANSLATIONAL MEDICINE 2018;7:569–582

SIGNIFICANCE STATEMENT

Skin therapeutic principles for local radiation-induced fibrosis/necrosis injury involve nonspecific medical/surgical interventions. The unpredictable spatio-temporal course of inflammatory waves due to skin irradiation makes conventional surgical treatment often ineffective. Wound healing often demands significant long-term medical attention, generally a maturation period of at least 6–18 months. Using a pig model, this study evaluated the long-term effects of bone marrow-derived mesenchymal stromal cell (BM-MSC) treatment on the preservation of wound-healing quality after surgical resection. All the specific surgical treatments of necrotic tissue resulted in a hypertrophic scar development and that, despite the placement of the vascularized flap, BM-MSCs treatment was required for remodeling to produce a lasting native dermal matrix and enabling vascular stability.

INTRODUCTION

Local, accidental, cutaneous overexposure to ionizing radiation has severe health consequences, especially when the absorbed dose exceeds 25 Gy and skin necrosis occurs [1]. Lesions can rapidly extend beyond the skin surface alone, involving underlying tissue (muscle and bone). The injury evolves by successive but unpredictable inflammatory waves over the first few days to weeks after irradiation, and these lead to horizontal and vertical extension of a process of full-thickness skin necrosis and ulceration [1]. Long-lasting cell dysfunction and stromal changes remain and impair cutaneous integrity.

Radiation-induced fibrosis and necrosis are usually considered intractable. Current therapeutic principles for local irradiation injury mostly involve nonspecific medical and surgical interventions with debridement of necrotic tissue, followed by different approaches including a skin graft, artificial derma application, or a rotation flap. Despite advances in modern plastic surgery techniques, such as skin grafting for the thermal injury, none has proved entirely satisfactory. The unpredictable spatiotemporal course of the substantial inflammatory waves due to irradiation makes conventional surgical treatment often ineffective or even harmful: every surgical procedure appears to stimulate inflammation and the fibronecrotic process [2]. In cases when healing is finally achieved, the scar remains fragile and unstable over time with a high risk of unpredictable upsurges.

Preclinical studies of wound healing have focused on mesenchymal stem cells (MSCs)—nonhematopoietic, adherent fibroblast-like cells with an intrinsic capacity for self-renewal and differentiation—as a possible cell population within the bone marrow that might contribute to cutaneous repair [3], particularly in radiation burns [4–8]. Optimum healing of skin wounds is orchestrated by several temporally processes that provide an anti-inflammatory effect, cell proliferation, control of the extracellular matrix (ECM) deposition, angiogenesis, and remodeling [9]. Impairment in this orderly progress of the healing process can lead to wound chronicity. The development of abnormal (e.g., hypertrophic or chronic) scarring may be one of the most common problems after radiation injury due to its functional consequences, especially when treatment includes surgery. Abnormal scars are probably due to overabundant collagen deposition—a cellular response by fibroblasts during the proliferation phase of wound healing [10]. MSC treatment strongly enhances scar quality, which some authors attribute to the greater quantity of collagen within the healed tissue, which increases its tensile strength [9, 11, 12]. The involvement of MSCs in the wound-healing process appears to be crucial in injuries resulting from irradiation exposure, especially for nonhealing wounds resulting from fibronecrosis. Some patients with severe radiological syndrome have been treated with autologous MSCs injection combined with surgery [13]. Most studies demonstrating the protective effects of MSCs [14] describe their short-term (i.e., within a month) protection, but data about long-term protection are sparse.

Wound healing often demands significant long-term medical attention and generally, a period of at least 6–18 months is required for maturation of burn scars [10]. Particularly in radiation burns the important questions concern long-term maintenance without inflammation and or renewed fibrosis. The healing process does not always go as planned, and some scars continue to remodel, grow, and expand, thereby becoming dysfunctional. Control of scar growth is thus important in clinical practice. Pigs are a preferred animal model for skin wounds, due to the similarity between their skin and human skin in architecture, structural epidermal thickness, dermal–epidermal thickness ratios, dermal collagen, and elastic content [15]. Pig skin wounds heal primarily by re-epithelialization rather than contraction, so they are especially useful in studying wound healing and burn lesions.

The aim of this study is to evaluate the long-term effects of bone marrow-derived mesenchymal stromal cell (BM-MSC) treatment on the preservation of wound-healing quality after surgical resection to treat cutaneous radiation overexposure. Our findings show that all the specific surgical treatments of necrotic tissue resulted in the development of a hypertrophic scar and that, despite the placement of the vascularized flap, BM-MSC was also required for remodeling to produce a lasting native dermal matrix.

MATERIALS AND METHODS

Animal Care

FBM minipigs, 12 months old and weighing about 20–25 kg (from La Ferme du Noyer, Bretoncelles, France), were placed in individual pens (21°C, 12-hour/12-hour light–dark schedule) in which they received solid food and had access to water ad libitum. All experiments were conducted in accordance with French regulations for animal experiments (Ministry of Agriculture Order No. A 78322-1, 2011).

Irradiation

Anesthetized (1.5% isoflurane in oxygen) animals received a high x-ray dose (Photon 4 MV, Linear Accelerator Alphee, IRSN, France). The total dose of 90 Gy was delivered in one external beam to the rump, in a $5*5$-cm^2 area. The beam field was aligned with the area to be irradiated by onboard lasers. Physical dosimetry was evaluated by thermoluminescent dosimeters, with alumina powder placed in the irradiated area.

Surgery and Cell Therapy

This study included 11 pigs: 3 irradiated pigs that underwent simple excision of the necrotic tissue and wound closure comprised the suture group, 4 irradiated pigs received a fasciocutaneous perforator flap (flap group), and 4 irradiated pigs received a fasciocutaneous perforator flap as well as repeated local administrations of autologous BM-MSCs (flap-MSC group). First, in all groups, 100–110 days after irradiation, the skin necrosis and underlying tissues up to healthy muscle were excised, and all deep fibrosis was removed until bleeding and muscle contraction occurred. In the suture group, the wound was closed by two large undermined skin flaps and absorbable suture. In the flap group, a magnifying lens was used to deepen the incision down into the muscle fascia and allowed us to identify one or more musculo- or septocutaneous perforators. The skin paddle was then designed and a pedicled fasciocutaneous perforator flap elevated. The elasticity of the surrounding skin allowed direct closure of the donor site with absorbable suture. In the flap-MSC group, the same surgical flap technique was supplemented with the cell therapy described below.

The cell therapy was delivered (from passage 0 of the first bone marrow collection, BM1, for details see the next subsection, Isolation, expansion, and characterization of clinical grade porcine MSCs) locally into the wound bed. Each injection consisted of 0.5–1 ml containing $5–10 * 10^6$ MSCs, for a total treatment dose of $50–72 * 10^6$ BM-MSCs. The first injection was performed in the muscle before that the flap was taken off to cover the entire wound. A second local administration of $50–72 * 10^6$ BM-MSCs (from passage 1 of BM1, volume 0.5–1 ml, $5–10 * 10^6$ BM-MSCs) took place around the flap and in the muscle under it 1 week after surgery. Similarly, the third and fourth MSC injections (passage 0 and 1 from BM2, see the next subsection) were injected 2 and 3 weeks after surgery (Fig. 1A). A piece of skin from animals in each treatment condition group (nonirradiated (C), irradiated (Irr), suture, flap without and flap with MSC treatment were sampled close to the scar at the time of surgery for the irradiated
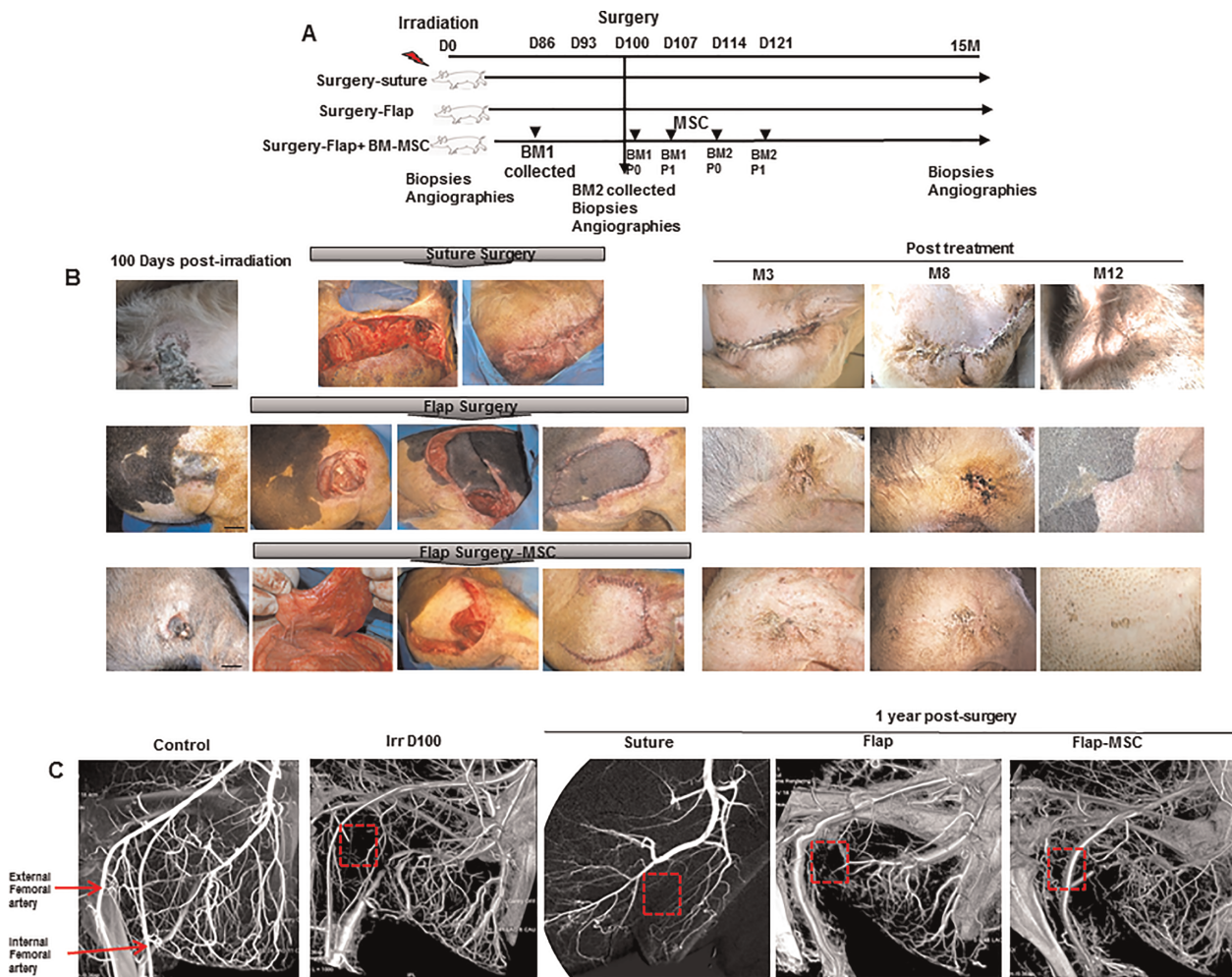
Figure 1. Clinical observation of defect coverage by healthy tissue, combined with BM-MSCs. **(A):** Experimental design. **(B):** Photographs at the day and after surgery for fibrosis/necrosis and kinetic of wound healing 12 months after suture surgery, vascularized-flap surgery, and vascularized-flap surgery with BM-MSCs treatment. The excision of the skin necrosis and suture or vascularized flap surgeries were practiced 100 days post-irradiation. The flap was taken off to cover the entire wound. In one group, the vascularized flap was combined with repeated local administrations of autologous BM-MSCs, one injection a week for 4 weeks. Scale bars: 5 cm. **(C):** Angiography showing the vascular network after irradiation and a year after treatment. Abbreviation: BM-MSCs, bone marrow-derived mesenchymal stromal cell.

group and 1 year after surgery and treatment for the suture, flap, and flap-MSC groups.

The Discovery* IGS 730 angiography system (GE Healthcare, France) was used to perform control angiographic examinations before irradiation, 1 day before surgery, and 1 year after surgery and treatment.

Isolation, Expansion, and Characterization of Clinical Grade Porcine MSCs

Bone marrow (30 ml) was collected from the humeral head of the pigs 12 days before injection, as previously described [16]. The four autologous BM-MSC transplantations required two humeral bone marrow collections (BM1 and BM2). Autologous bone marrow mononuclear cells (BM-MNCs) were expanded in a clinical-grade BM-MSC production process that used 636 cm^2 closed culture devices (Cellstacks, Macopharma, Tourcoing, France) and were seeded at 100,000 cells/cm^2 in GMP minimal essential medium α (α-MEM, Macopharma) supplemented with 10 μg/ml ciprofloxacin (200 mg/100 ml,

Aguettant, Lyon, France) and 20% fetal bovine serum (A15–101 PAA, France). After 3–4 days, nonadherent cells were removed and cultures were refed with fresh medium. Thereafter, cultures were fed twice a week, and the adherent fibroblast-like cells (passage 0) were cultured for 2–3 weeks. At that time, they were detached by using recombinant bovine trypsin expressed in corn (Trypzean, Sigma-Aldrich, USA) and numerated by Trypan blue staining. Cells were suspended in a saline solution (0.9% NaCl) supplemented with 0.4% final human albumine (LFB, France) prior to animal administration.

Proliferative Capacity. The number of BM-MSC was evaluated at 3 weeks (end of P0) obtained from BM-MNCs seeded at 100,000 cells/cm^2 by cell culture unit (Cellstacks). Some of the cells were plated at 4,000 cells/cm^2 in new cell culture chambers (passage 1) and allowed to grow for 1 week, until they reached 80%–90% confluence. The proliferation capacity at P1 was determined using the following formula: (N collected in end p1/N plated in beginning p1) * total N obtained in end p0 where N is the number of BM-MSC.

Colony-Forming Unit Fibroblast Assays. To evaluate the potential of MSCs to form colonies, BM-MNCs were plated at 330,000 cells per 25-cm^2 flask at P0 and MSCs were plated at 200 cells per 25-cm^2 flask at P1, to verify the maintaining of the progenitor capacity. Cells were cultured for 10 days before ethanol fixation, Giemsa staining, and colony number recording.

Flow Cytometry. Expression of MSC markers was studied by fluorescence-activated cell sorting. Cells were stained with CD90-PE (clone 5E10; BD Pharmingen), CD44-PE (clone MEM-263; Abcam), CD29-FITC (clone MEM-101A; Abcam), swine leukocyte antigen SLA1-FITC (clone JM1E3; AbD Serotec), CD105-PE (clone MEM-229; Abcam), and CD45-FITC (clone 1E4; AbD Serotec) antibodies. FITC- or PE-conjugated isotype antibodies (clone W3/25; AbD Serotec) were included as controls. Cell staining was analyzed on a Facscalibur Cytometer (Becton Dickinson).

Differentiation Assays. For osteogenic differentiation, porcine MSCs were grown for 14 days in α-MEM supplemented with 100 nM dexamethasone (Sigma), 10 mM β-glycerophosphate (Sigma), 0.05 mM ascorbic acid (Sigma), 10 mg/ml ciflox, and 10% FBS (PAA). A colorimetric assay (Vector Blue Alkaline Phosphatase Substrate Kit III; Vector Laboratories) was used to detect alkaline phosphatase activity. Alizarin red S and von Kossa staining (Sigma) were used to identify mineralized bone matrix deposition in cells. To evaluate adipogenic differentiation capacity, cells were grown in basal medium supplemented with 5 ng/ml epidermal growth factor (EGF), 0.5 ng/ml vascular endothelial growth factor (VEGF), 10 ng/ml fibroblast growth factor 2 (FGF2), 20 ng/ml Insulin-like growth factor-1 (IGF1), 0.2 μg/ml hydrocortisone, 1 μg/ml ascorbic acid, 22.5 μg/ml heparin, 1 X antibiotics (gentamicin and amphotericin B), and 2% fetal bovine serum (FBS) (Lonza). After 3 weeks, fixed cells were incubated with an oil red O solution (lipid droplet assay, Cayman Chemical) before examination. Chondrogenic differentiation was induced in cell masses in DMEM high glucose medium (Gibco) supplemented with 100 mM dexamethasone, 1 mM sodium pyruvate, 0.17 mM ascorbic acid, 0.35 mM L-proline, 1 X insulin-transferrin-selenium (Sigma), 5.33 μg/ml linoleic acid (Fluka), 1.25 mg/ml human albumin (LFB), 10 mg/ml ciflox, and 10% FBS (PAA). After 21 days, cell masses were fixed, embedded, and sectioned with a microtome. Acidic mucopolysaccharides were stained with alcian blue solution to demonstrate cartilage matrix production.

Histological and Immunohistochemical Analysis

Freshly isolated skin biopsies from the irradiated area at the time of surgery and close to the scar 1 year after surgery and treatment were fixed in 4% paraformaldehyde and embedded in paraffin. Sections 5 μm thick were dewaxed and hydrated; endogenous peroxidase was blocked with 3% hydrogen peroxide for 10 minutes; and nonspecific binding was blocked with a protein blocker (DakoCytomation, Trappe, France). H&E cross-sections staining were used to evaluate epidermal and dermal thicknesses and the collagen fibers diameter in the dermis reticular layer. Dermal thickness was measured as the distance between epidermal and dermal-adipose layer junction. A total of five measurements were performed from regions of interest generated randomly from the entire skin section using the image analysis software Histolab (Microvision Instruments; France). Collagen deposition was detected by Sirius red staining according to standard methods. A

heat-induced epitope retrieval pretreatment method was used for the primary Col3a (Ab7778), tenascin C (TNC) (Ab108930), and S100A4 (Ab27957) antibodies and pretreatment with proteinase K (DakoCytomation) for monocyte/macrophage MAC387 (Thermo Fisher Scientific), α-SMA (Ab5694), and Von Willebrand factor antibodies (A0082, Dako). The EnVision$^+$ System (horseradish peroxidase) (DakoCytomation) was used as a secondary reagent for all immunostained sections. The color reaction was developed with the NovaRED kit (Vector Laboratories, Inc., Burlingame, CA) and counterstained with Meyer's hemalun. For Von Willebrand factor, staining was developed with Histogreen substrate (E109; Abcys) and sections were counterstained with Fast nuclear red (H-3403; Vector). α-SMA immunofluorescence staining was performed with goat anti-rabbit Alexa 568 (Molecular probes). Cell nuclei were counterstained by Vectashield mounting medium with DAPI (Vector Laboratories).

TUNEL Detection Assay. To analyze the degree of skin apoptosis, terminal deoxynucleotidyl transferase dUTP nick end labeling (TUNEL) immunostaining was performed with the In Situ Cell Death Detection Kit, POD (Roche, Alameda, CA), according to the manufacturer's instructions.

Matrix Metalloproteinases Immunoassays

Total proteins were obtained by skin homogenization in cold PBS containing a standard protease-inhibitor cocktail. The samples were then centrifuged at 10,000*g* for 10 minutes, and the supernatants stored at −20°C for later measurement. The MMP-2 assay used ELISA kits (R & D Systems, France) according to the manufacturer's instructions. Results are expressed as the mean (±SEM) ng/μg protein after a protein assay with a Pierce BCA protein assay kit.

Matrix Metalloproteinase Activity Assays

Gelatinase activity (MMP2/MMP9) was measured in skin homogenates by fluorometry, with a Molecular Probes EnzChek Gelatin assay kit (Invitrogen Corporation, France). The assay was performed according to the manufacturer's recommendations, and the fluorescent intensity was measured with a spectrofluorometer. Data were expressed as matrix metalloproteinase (MMP) activity in arbitrary units per μg protein.

Real-Time PCR Analysis

Total RNA was extracted from skin with the RNeasy Mini kit (Qiagen), and cDNA was prepared with the SuperScript RT Reagent Kit (Applied Biosystems). Real-time PCR was performed on an ABI Prism 7000 Sequence Detection System. SYBR chemistry (Life Technologies) was used to amplify PCR, with the specific primers listed in Table 1. All other Taqman primers and probes came from Life Technologies. Data were analyzed by the $2^{-\Delta\Delta Ct}$ method [17], with normalization to the Ct of the housekeeping gene glyceraldehyde 3-phosphate dehydrogenase.

Cell Wound Healing Assay

Fibroblasts from the nonirradiated and irradiated cutaneous biopsies were harvested with buffered EDTA, resuspended in serum-free DMEM with 0.1% BSA, and plated into 12-well culture plates (3×10^4 cells/well). The fibroblasts were cultured at confluence in DMEM (Invitrogen, France) culture medium, supplemented with 10% FBS and antibiotics (penicillin/streptomycin, Invitrogen) at 37°C and in a humidified atmosphere

Table 1. Swine primers for real-time PCR

	Forward	Reverse
IL-6	5′-ATCAGGAGACCTGCTTGATG-3′	5′-TGGTGGCTTTGTCTGGATTC-3′
TNF-α	5′-CCAATGGCAGAGTGGGTATG-3′	5′-TGAAGAGGACCTGGGAGTAG −3′
Col1a2	5′- CAGAACGGCCTCAGGTACCA-3′	5′-CAGATCACGTCATCGCACAAC-3′
Col3a1	5′CCTGGACTTCCTGGTATAGC-3′	5′-TCCTCCTTCACCTTTCTCAC-3′
TGF-β1	5′-GCACGTGGAGCTATACAGA-3′	5′-ACAACTCCGGTGACATCAAA-3′
MMP2	5′-TCCTGGGCTGCCTGTTGG-3′	5′-TGGGGCAGCCGTAGAAGGT-3′
MMP3	5′-AGTGACTCCGCTTACATTCTCC-3′	5′-TTTCCAGGTCCGTCAAAAGGG-3′
MMP9	5′-AAGACGCAGAAGGTGGATTC-3′	5′-AACTCACACGCCAGAAGAAG-3′
TIMP1	5′-GAGCCCCAGAGTTCAACCAGAC-3′	5′-GGCGGGGGCGTAGATGA-3′
TIMP2	5′-AGGGGCACGGCAAGATG-3′	5′-CAGGGGATCATGGGACAGC-3′
eNos	5′-GGCATCGCCAGAAAGAC-3′	5′-CATCACGGTGCCCATGAGT-3′
VEGF	5′-CCATGCAGATTATGCGGATCA-3′	5′-TCTCTCCTATGTGCTGGCCTTG-3′
GAPDH	5′-GACCCCTTCATTGACCTCCAC-3′	5′-TCCCATTCTCAGCCTTGACTG-3′

Abbreviations: eNos, endothelial nitric oxide synthase; GAPDH, glyceraldehyde 3-phosphate dehydrogenase; PCR, polymerase chain reaction; VEGF, vascular endothelial growth factor.

Table 2. Characteristics of BM-MSC isolation

	Run	
	P0	P1
Cell doubling time (days)	1.44	1.6
Average expansion rate	0.75	24.6
Culture duration (days)	15	7
CFU-F efficiency (%)	0.002	14.8
Mycoplasma contamination	Negative	Negative
Telomerase activity	Negative	Negative

Extraction yield = 36.5×10^6 BM-MNCs per milliliter of bone marrow. Abbreviations: BM-MNC, bone marrow mononuclear cells; BM-MSC, bone marrow-derived mesenchymal stromal cell; CFU-F, colony-forming unit-fibroblast.

containing 5% CO_2. The fibroblast monolayers were then scratched with a sterile pipette tip to leave a linear scratch approximately 0.3–0.4 mm in width. Transwell inserts (Corning, France) were added to fibroblasts containing BM-MSC at confluence. Wound closure was monitored by collecting digitized images at various time intervals after the scratch. The amount of wound closure was calculated as the mean percentage of the migrated distance compared with the initial wound distance.

STATISTICS

Data are expressed as means ± SEM. We used one-way analysis of variance and then a Bonferroni post-test to determine the significance of differences. p values less than .05 were considered statistically significant.

RESULTS

BM-MSC Characterization

The pig BM-derived-MSCs presented a characteristic spindle shape and reached confluence by day 14 at passage 0 and day 7 at passage 1 (Table 2). Colony-forming unit-fibroblast assays indicated that the percentage of colonies was about 0.002% during P0 and 14.8% in P1. Flow cytometry analysis at P1 showed that cells were positive (>90%) for CD90, CD29, CD44, and SLA-1 surface markers and cells differentiated into adipocytes, osteoblasts, and chondrocytes when cultured in medium that was simultaneously osteogenic, adipogenic, and chondrogenic (Supporting Information Fig. S1).

BM-MSC Injections Promoted Recovery of the Wound Caused by Severe Irradiation

The clinical course of these lesions in pigs is similar to that observed in humans and characteristic of cutaneous radiation. Transient erythema appeared, followed first by a clinically silent period and then the onset of dry desquamation at 2 months and skin necrosis by 3 months, without healing (Fig. 1B). All pigs in the suture group evolved toward early recurrence of radionecrosis within 21 days of surgery, with a chronic ulcerated lesion. Finally, healing was observed at 8 months after surgery, but the scar was atrophic, and integument of the posterior face of the thigh retracted. The flap surgery performed (in both the flap and flap-MSC groups) resulted in good vitality of the flap, which healed with the sutures. But in the flap-MSC group, the coverage was stable over time, with no recurrence of the radiation injury during the 12-month post-surgery follow-up; the flaps were perfectly integrated in their recipient sites, whereas in the flap group necrosis recurred at 3 months and was still seen 12 months later.

The depth of irradiated musculocutaneous area was confirmed by angiographic analysis, with the vascular network between the superficial external and internal (deep) femoral artery drastically decreased, compared with the nonirradiated group (Fig. 1C). At 1 year, the suture group showed no improvement in the vascular network. Nor was the vascular network restored in the flap group, and a structure of the diameter of internal femoral artery was observed. Although not totally restored, the MSC treatment resulted in a greater vascular network than in the flap group without MSCs. Together these clinical results suggest that covering the
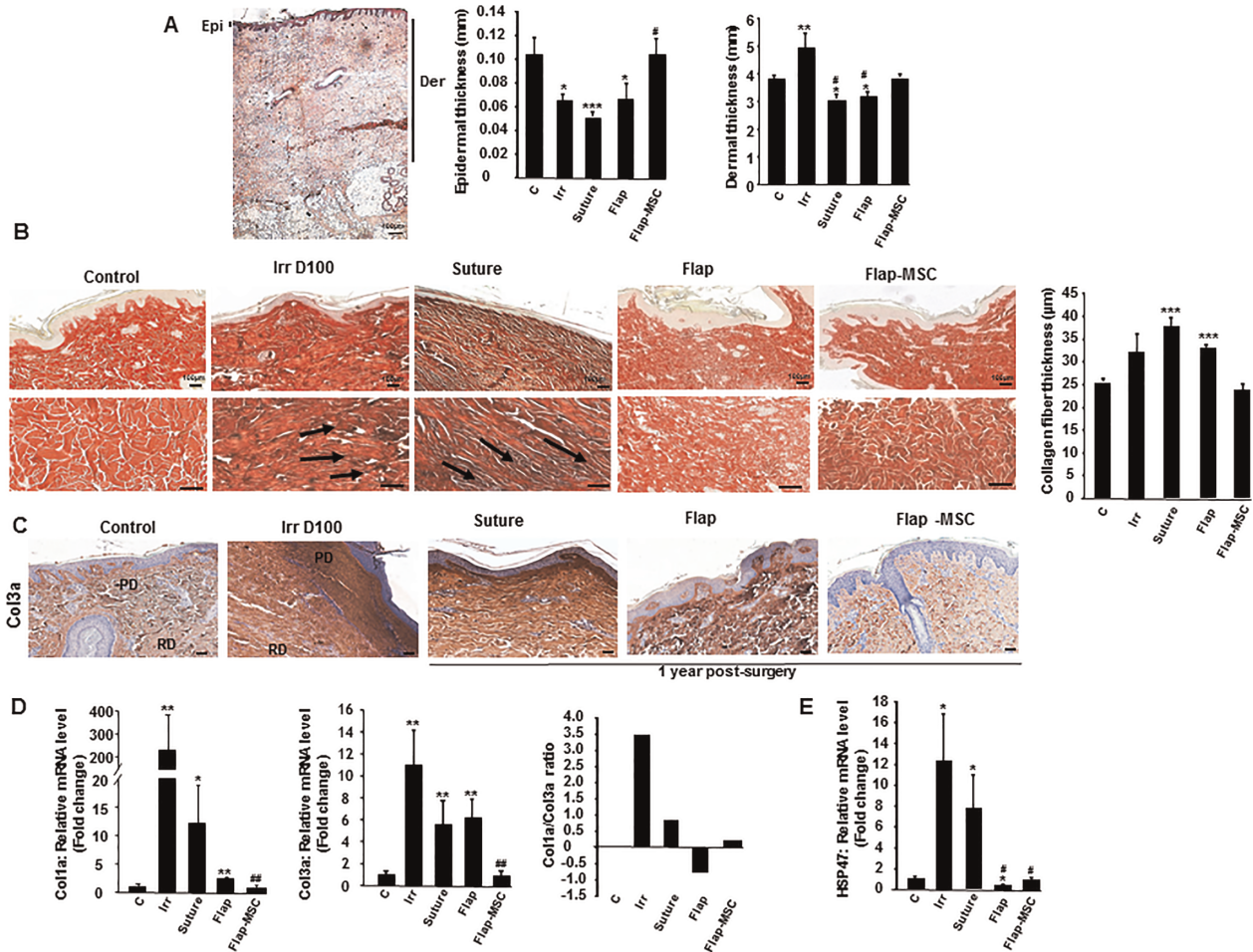
Figure 2. Flap surgery, with and without autologous bone marrow-derived mesenchymal stromal cells, modified radiation-induced collagen deposition. **(A):** Histopathological analysis of the epidermal and dermal thicknesses: Representative H&E staining of nonirradiated skin and quantification of epidermal and dermal thicknesses. **(B):** Red Sirius staining and measure of collagen fiber thickness in nonirradiated skin (control group), irradiated skin on the day of surgery (Irr group), and 12 months after resection (suture group), flap surgery without (flap group) and with MSC treatment (flap-MSC group). Staining revealed a high density of dermal collagen fibers with unidirectional alignment parallel to the black arrows after irradiation and without treatment and the restoration of multidirectional alignment after flap surgery without and with MSC treatment. **(C):** Col3a staining. Real-time-PCR of **(D)** Col3a, Col1a, and the Col1a/Col3a ratio, and **(E)** HSP47. Data are expressed relative to control skin and normalized to glyceraldehyde 3-phosphate dehydrogenase. Results are expressed as means ± SEM. p values were calculated by analysis of variance with Bonferroni correction, *, $p < .05$; **, $p < .01$; ***, $p < .001$ compared with nonirradiated skin; #, $p < .05$; ##, $p < .01$ compared with irradiated-untreated control. Scale bars: (A) = 400 μm; (B, C) = 100 μm. Abbreviations: Der, dermal; Epi, epidermal; MSC, mesenchymal stromal cell; PD, papillary dermis; RD, reticular dermis; PCR, polymerase chain reaction.

defects by healthy tissue while simultaneously injecting MSCs accelerates and maintains the healing process.

BM-MSC Injections Reduced Collagen and HSP47 Expression

The presence of collagen within the ECM is responsible for the strength and resiliency of skin, and it mediates effective wound healing. First, histological analysis of skin section showed a marked reduction of the epidermal thickness and an increase of the dermal thickness at the day of the surgery. In both suture and flap groups, the epidermal and dermal thicknesses were not restored 1-year post-surgery when they were normalized in the flap-MSC group compared with nonirradiated skin (Fig. 2A).

In nonirradiated skin, the tissue sections stained with Sirius red dyes showed the presence of an undulating dermal-epidermal junction and skin appendages (Fig. 2B). One-year post-

surgery, the epidermis of the suture group showed flattened rete ridges. The dermis contained a high density of collagen fibers with unidirectional alignment, and atrophy of the dermal appendages, similar to the irradiated skin the day of surgery (day 100). On the contrary, both flap groups, with and without MSCs, showed restored epidermal rete ridges, multidirectional alignment (remodeling) of collagen fibers, and dermal appendages, similar to that of nonirradiated skin. But only in the flap-MSC group was the thickness of collagen fibers restored to a level similar to that of nonirradiated skin.

To assess the differences in collagen between groups, we measured the expression level of Col1a and Col3a in tissue samples with real-time PCR. First, Col3a immunostaining showed very intense staining in the dermis with marked staining localized in the papillary dermis of the suture and flap groups, similar to that of irradiated skin at the time of surgery (Fig. 2C). Only the flap-MSC group showed a net reduction in
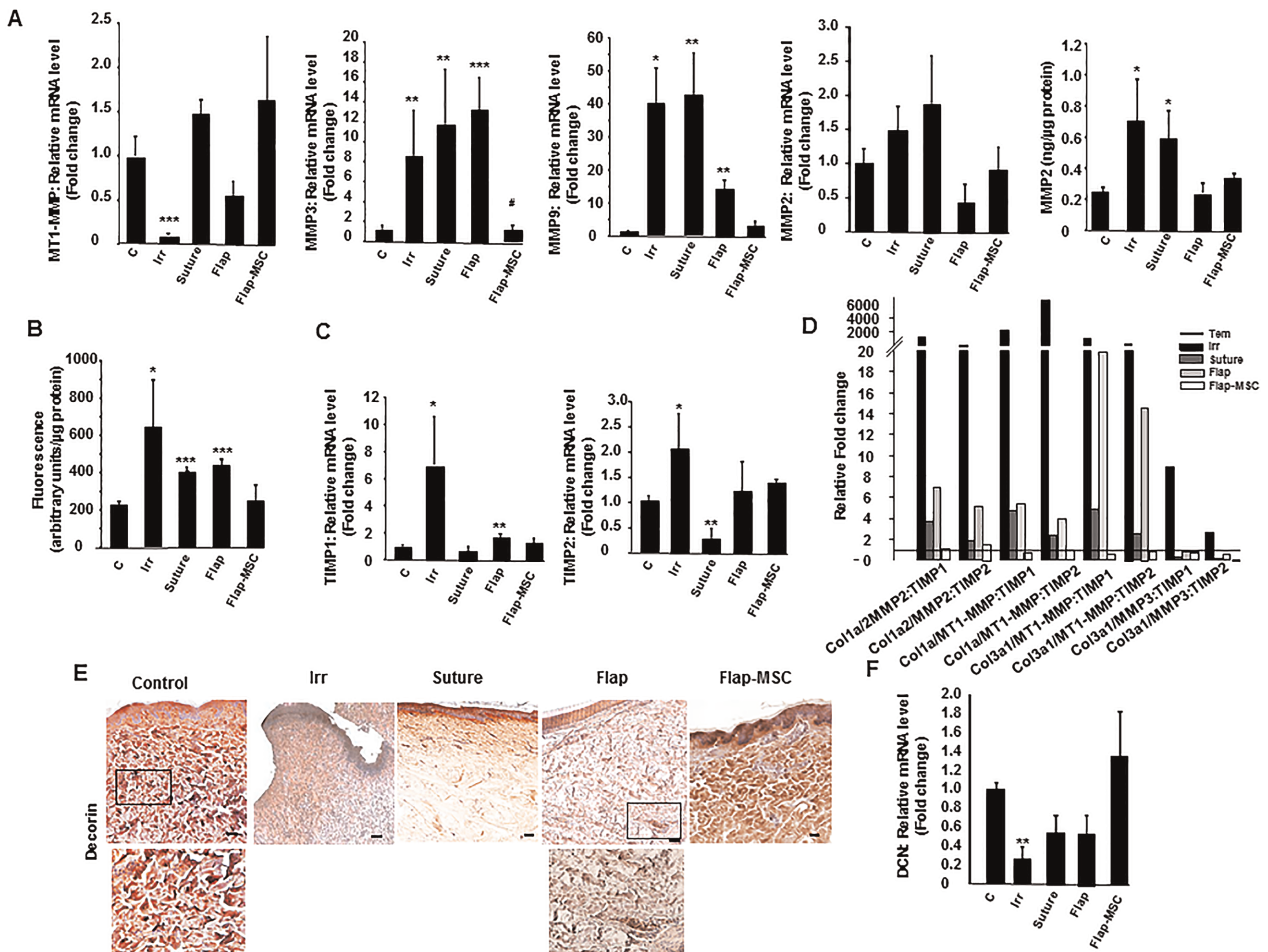
Figure 3. Bone marrow-derived mesenchymal stromal cell treatment associated with flap surgery influenced extracellular matrix remodeling. **(A):** Real-time expression of MT1-MMP, MMP-3, MMP-9, and MMP-2 (gene and protein). **(B):** Activity of matrix metalloproteinases (MMPs). **(C):** mRNA expression of TIMP-1 and TIMP-2. **(D):** Collagen-to-MMP-to-TIMP ratio: Relative expression of MMP was calculated by determining the fold-change of MMP mRNA levels relative to the relevant TIMP in irradiated skin on the day of surgery, in the suture, flap, and flap-MSC groups compared with the control group. **(E):** Representative immunohistochemical decorin staining of skin section from the control group, an irradiated pig on the day of surgery, and the suture, flap and flap-MSC groups a year after surgery. **(F):** Real-time PCR of decorin. Results are expressed as means ± SEM. p values were calculated by analysis of variance with Bonferroni correction, *, $p < .05$; **, $p < .01$; ***, $p < .001$ compared with nonirradiated controls; #, $p < .05$ compared with irradiated group on the day of surgery. Scale bars: 100 μm. Abbreviations: MSC, mesenchymal stromal cell; TIMPs, tissue inhibitors of metalloproteinases; PCR, polymerase chain reaction.

Col3a staining. As Figure 2D shows, significant increases in mRNA levels of both Col1a (250-fold, $p < .01$) and Col3a (11-fold, $p < .01$) were detected in irradiated tissue the day of surgery, compared with nonirradiated skin. The suture surgery modestly reduced Col1a and Col3a overexpression. Col1 expression fell significantly more after the flap surgery, but remained elevated compared with nonirradiated skin (2.5-fold, $p < .01$) and showed no major reduction in Col3a overexpression. In the flap-MSC group, however, levels of Col1a and Col3a expression were restored and again similar to those in nonirradiated skin. The resulting ratio of collagen 1/3, as an indicator of tissue quality, confirmed that this ratio returned to normal level only in the flap-MSC group.

Some reports have shown that heat-shock protein HSP47, a collagen-specific intracellular chaperone, plays a specific role in the modification and assembly of collagen [18] and in the development of fibrosis by promoting collagen accumulation [19]. Compared with nonirradiated skin, HSP47 was overexpressed (12-fold, $p < .05$) in irradiated skin on D100, the day of

surgery (Fig. 2E). The suture surgery did not reduce this overexpression significantly. On the other hand, the level of HSP47 mRNA was significantly downexpressed in flap-group skin and normalized in flap-MSC skin, that is, similar to that in the nonirradiated skin.

Together, these data showed that despite the normal appearance of the epidermis observed after flap surgery, only in the group with both flap surgery and MSC treatment were the nature and structure of these two collagen fibers again similar to those of nonirradiated skin.

BM-MSC Injections Modulated MEC Remodeling

MMPs are also involved in tissue repair and remodeling processes where an imbalance in their activity is often associated with chronic impairment of wound healing [20]; TIMPs, are the endogenous tissue inhibitors of metalloproteinases. Therefore, we sought to assess the expression levels of various MMPs and TIMPs in the wound tissue of treated animals. On the day of surgery, RT-PCR revealed significant modification of
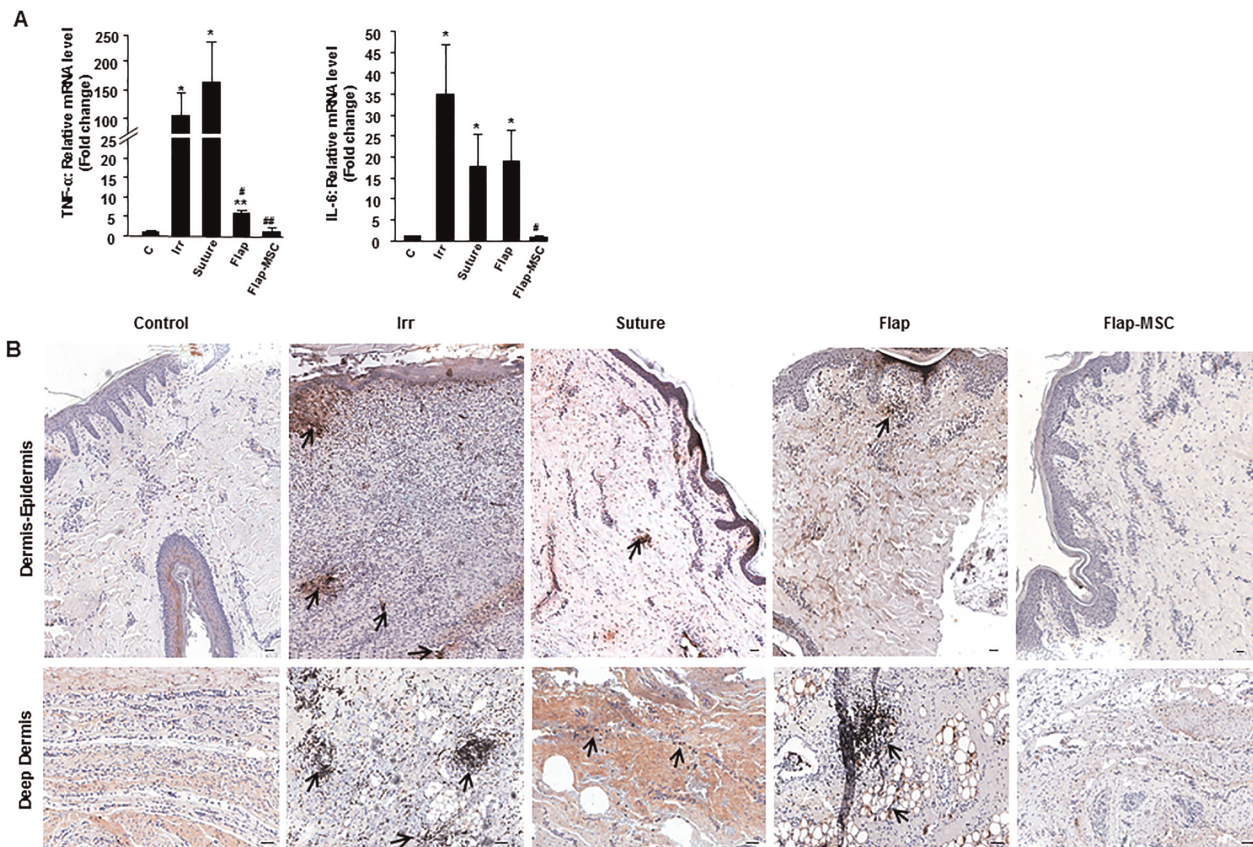
Figure 4. Modification of inflammatory profile in group with flap surgery and bone marrow-derived mesenchymal stromal cell therapy. **(A)**: Real-time-PCR analysis of TNF-α and IL-6. **(B)**: Representative immunostaining for MAC387-positive macrophages in the epidermis-dermis and deep dermis of nonirradiated, irradiated on the day of surgery, and suture, flap, and flap-MSC groups a year after surgery. Arrows indicated the presence of macrophages. Scale bars: 100 μm. Results are expressed as means ± SEM. p values were calculated by analysis of variance with Bonferroni correction, *, $p < .01$; **, $p < .001$ compared with nonirradiated controls; #, $p < .05$; ##, $p < .01$ compared with irradiated controls. Abbreviations: MSC, mesenchymal stromal cell; PCR, polymerase chain reaction.

MMPS in the irradiated tissue, with reduced levels of MT1-MMP and increased levels of MMP3 and MMP9 (Fig. 3A). MT1-MMP expression was fully reestablished in all groups 1 year after treatment, whereas the overexpression of MMP3 and −9 fell back toward normal only in the flap-MSC group. MMP2 expression (gene and protein) increased (protein expression significantly) in the irradiated skin and suture groups, but returned to normal levels in both flap groups. Analysis of gelatinase activity (MMP-2,-9) in skin showed higher MMP activity in irradiated skin the day of surgery than in nonirradiated skin (Fig. 3B). This activity remained elevated in the surgery groups (suture and flap groups) without MSC treatment. Expression of both Timp-1 and −2 increased significantly in the irradiated tissue (Fig. 3C), and only in the flap-MSC group did both Timp-1 and −2 return to normal levels. Because collagen synthesis/degradation depends on the dynamic interactions of MMPs and TIMPs, their relations were assessed by the collagen-to-MMP-to-TIMP ratio, a method of defining net collagen deposition [21] that assumes a ratio of one at baseline (here, the nonirradiated skin). Real-time PCR results of the irradiated groups showed that only in the flap-MSC group was this ratio again close to 1 (Fig. 3D).

Decorin is the most abundant proteoglycan in normal dermis; it defines and delimits the fibril surface and promotes the lateral association of collagen fibrils to form fibers and fiber-bundles. Because decorin deficits lead to a delay in cutaneous wound healing [22], we examined its expression level in this animal model. The nonirradiated dermis showed strong staining for decorin, which was associated with collagen fibers (Fig. 3E). On the day of surgery, the irradiated skin showed very little decorin staining or association with cells. A year later, staining had increased in the papillary dermis of the suture group, but very weakly, and had spread out in the flap skin. In the flap-MSC skin, however, staining was much more important and closely resembled that in nonirradiated skin. Real-time PCR analysis confirmed the significant downregulation—by about 75% ($p < .001$)—of decorin expression in the irradiated compared with nonirradiated skin (Fig. 3F). Although not significant, decorin expression decreased by 40% in the suture and flap groups, while in the flap-MSC group it was similar to that in nonirradiated skin. Together these results showed that MSC treatment associated with the flap surgery restored levels of matrix proteins involved in healing.

Fibroblast Activation Depends on Inflammation

Given that the wound repair process is likely to be influenced by inflammation, particularly late in the regenerative or resolving phases when it may induce continued remodeling and excessive scarring [23], we studied the levels of inflammatory cytokines in the wound area. On the day of surgery, expression
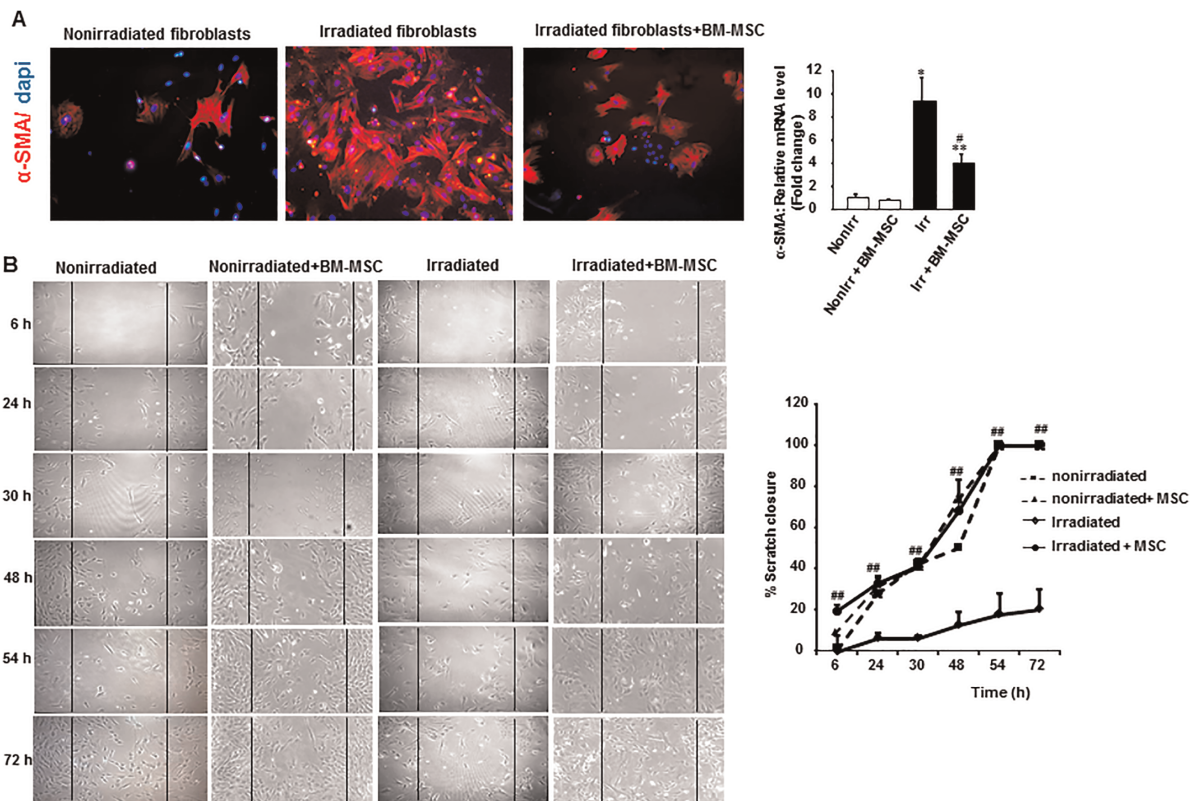
Figure 5. BM-MSC therapy enhanced migration of nonirradiated and irradiated fibroblasts from skin biopsy samples. Fibroblasts were plated to confluence and mechanically "wounded" by scraping with a 200 μl pipette tip. Transwell inserts were added to fibroblasts containing BM-MSCs at confluence. **(A):** Representative α-SMA immunostaining of nonirradiated and irradiated fibroblasts cocultured 24 hours with BM-MSCs. Image magnification ×200. **(B):** Representative photomicrograph of the wound edge in the scratch assay at 6, 24, 30, 48, and 72 hours without and with MSC coculture. MSC significantly enhanced migration in both nonirradiated and irradiated fibroblasts. The migration rate is represented as percent scratch closure. Results are expressed as means ± SEM. p values were calculated by analysis of variance with Bonferroni correction, *, $p < .01$; **, $p < .001$ compared with nonirradiated controls; #, $p < .05$; ##, $p < .01$ compared with irradiated fibroblasts. Abbreviations: α-SMA, alpha smooth muscle actin; BM-MSC, bone marrow-derived mesenchymal stromal cell; MSC, mesenchymal stromal cell.

of the inflammatory cytokines TNF-α and IL-6 was significantly elevated, about 100- and 36-fold ($p < .01$), compared with nonirradiated skin (Fig. 4A). At the end of a year, TNF-α and IL-6 expression remained significantly elevated in the suture and the flap surgery groups. In contrast, the group with MSC injections and flap surgery had inflammatory cytokine levels similar to those of nonirradiated skin. MAC387 immunostaining showed increased macrophage density in the dermis with some important foci near the hypodermis in the irradiated skin, while staining was infrequent in nonirradiated skin (Fig. 4B). In both the suture and flap groups, the stained macrophages, albeit less marked, remained positive throughout the entire depth of the dermis. In the flap-MSC group, staining showed sparse MAC387-positive macrophages, similar to nonirradiated skin.

BM-MSCs Controlled the Accumulation of Fibroblasts/Myofibroblasts in the Matrix During Wound Resolution

Attenuating myofibroblast differentiation and reducing collagen deposition and matrix production promotes ECM remodeling [24]. First, to determine whether BM-MCSs can regulate the phenotype and activity of irradiated fibroblasts, the two were cocultured. Immunostaining, confirmed by real-time PCR analysis, showed that BM-MSCs decreased α-SMA expression

by irradiated fibroblasts (Fig. 5A). In addition, we used the scratch assay method to test the ability of BM-MSCs to induce fibroblast migration during the wound-healing process (Fig. 5B). In the presence of BM-MSCs, the migration of nonirradiated fibroblasts accelerated: wound closure reached 50% after 30 hours of coculture, compared with the 48 hours required for fibroblasts without MSCs. Similarly, the migration rate of irradiated fibroblasts increased significantly in the presence of BM-MSCs and reached 50% wound closure at 30 hours of coculture; although the irradiated fibroblasts alone (without BM-MSCs) only attained 20% of wound closure at 72 hours. Accordingly, BM-MSCs enhanced the migration rate by reducing the myofibroblast phenotype.

In chronic remodeling and fibrosis, fibroblasts are aberrantly activated to myofibroblasts, which results in excessive ECM deposition, standard fibroblast activation, on the other hand, is part of the normal wound healing response [25]. Accordingly, we used immunohistochemical staining for α-SMA and S100A4 (so-called FSP1) to examine the prevalence of myofibroblasts and activated fibroblasts, respectively. In the nonirradiated skin, the α-SMA staining (Fig. 6A) was essentially close to blood vessel walls, and low-level S100A4 staining (Fig. 6B) was homogenous in the dermis. On the day of surgery, all vertical layers of the dermis stained intensely positive
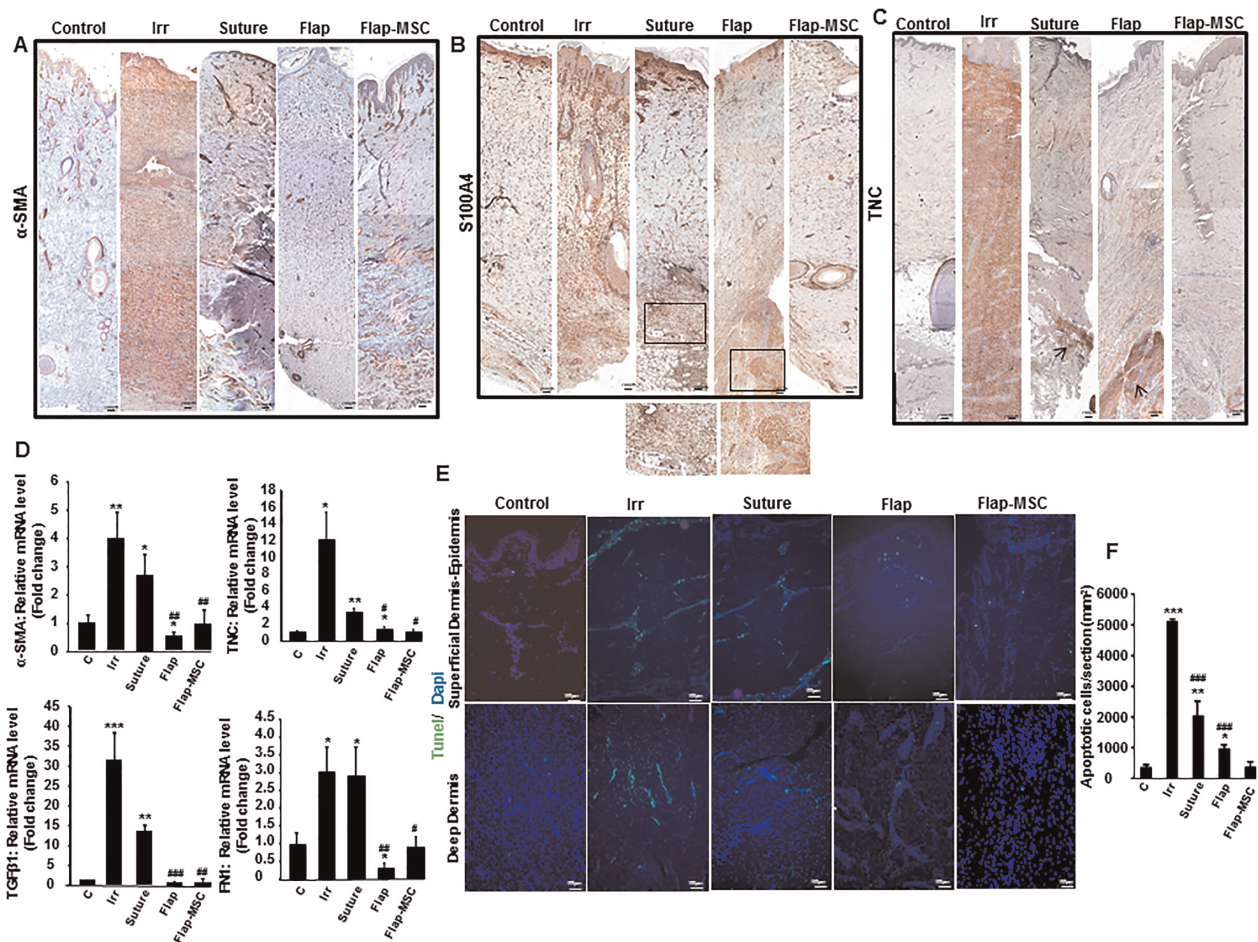
Figure 6. Bone marrow-derived mesenchymal stromal cells controlled the fibroblast/myofibroblast accumulation. **(A):** Representative immunostaining of α-SMA, an indicator of myofibroblasts showed a staining around the vessels in nonirradiated, suture, flap and flap-MSC groups and homogenous in the dermis (dark red) in irradiated group. **(B):** S100a4, a marker of activated fibroblasts, better illustrated in the magnified view in the box (dark red staining), and **(C)** TNC, an indicator of wound healing throughout the dermis. The TNC staining was intensely homogenous in irradiated group and arrows showed some dark red foci staining in the deep dermis in suture and flap groups. Scale bars: 200 μm. **(D):** Real-time expression of wound healing-related factors, α-SMA, TNC, and FN1 (fibronectin). **(E):** TUNEL staining was performed to determine apoptosis. **(F):** Cellular apoptosis quantification. Scale bars: 100 μm. Results are expressed as means ± SEM. p values were calculated by analysis of variance with Bonferroni correction, *, $p < .05$; **, $p < .01$; ***, $p < .001$ compared with nonirradiated controls; #, $p < .05$; ##, $p < .01$; ###, $p < .001$ compared with irradiated controls. Abbreviations: α-SMA, alpha smooth muscle actin; MSC, mesenchymal stromal cell; TNC, tenascin C; TUNEL, Terminal deoxynucleotidyl transferase dUTP nick end labeling.

for both α-SMA and S100A4. A year later, the α-SMA staining in the suture group remained strong in myofibroblasts, blood vessels, and fine collagen, producing a "tram track" appearance. Inversely, only a few α-SMA-positive cells were observed in the flap, mainly located around the blood vessels, while in the flap-MSC group, α-SMA staining around the vessels was similar to that of nonirradiated skin. S100A4 immunostaining was positive in the dermis and quite notable in the papillary dermis of irradiated skin the day of surgery. At the end of the year, S100A4 staining in the suture and flap groups was observed in the deep dermis near the hypodermis and concentrated in a nodule, while in the flap-MSC group, it was close to the vessels and similar to that in nonirradiated skin.

It has previously been reported that tenascin-C expression is transient [26], occurring and at high levels only during wound healing and not present in either unwounded or healed tissue. Its persistence promotes fibrosis. On the day of surgery, immunostaining showed "mirror" S100A4 staining, with intense tenascin-C staining throughout the dermis, while it

was largely absent in nonirradiated skin. This tenascin-C staining decreased after surgery (suture and flap) but nonetheless remained intense in the deep dermis; it was absent in the flap-MSC group (Fig. 6C).

The differentiation of fibroblasts into myofibroblasts depends on profibrogenetic factors, mainly TGF-β1, and the presence of specialized matrix proteins, such as fibronectin [27]. Accordingly, real-time PCR analysis confirmed the overexpression of α-SMA, TNC, TGF-β1, and fibronectin (FN1) in skin on the day of surgery as well as its maintenance at significantly elevated levels after the suture surgery (Fig. 6D). In the flap group, compared to nonirradiated skin, α-SMA, TGF-β1, and FN1 expression were downregulated while TNC remained significantly increased. On the contrary, the expression of all returned to normal levels in the flap-MSC group.

Cellular apoptosis was assayed by TUNEL staining (Fig. 6E), because apoptosis is a mechanism of myofibroblast resolution. Thus, on the day of surgery, TUNEL staining showed a large number of apoptotic cells in epidermis-papillary dermis and in
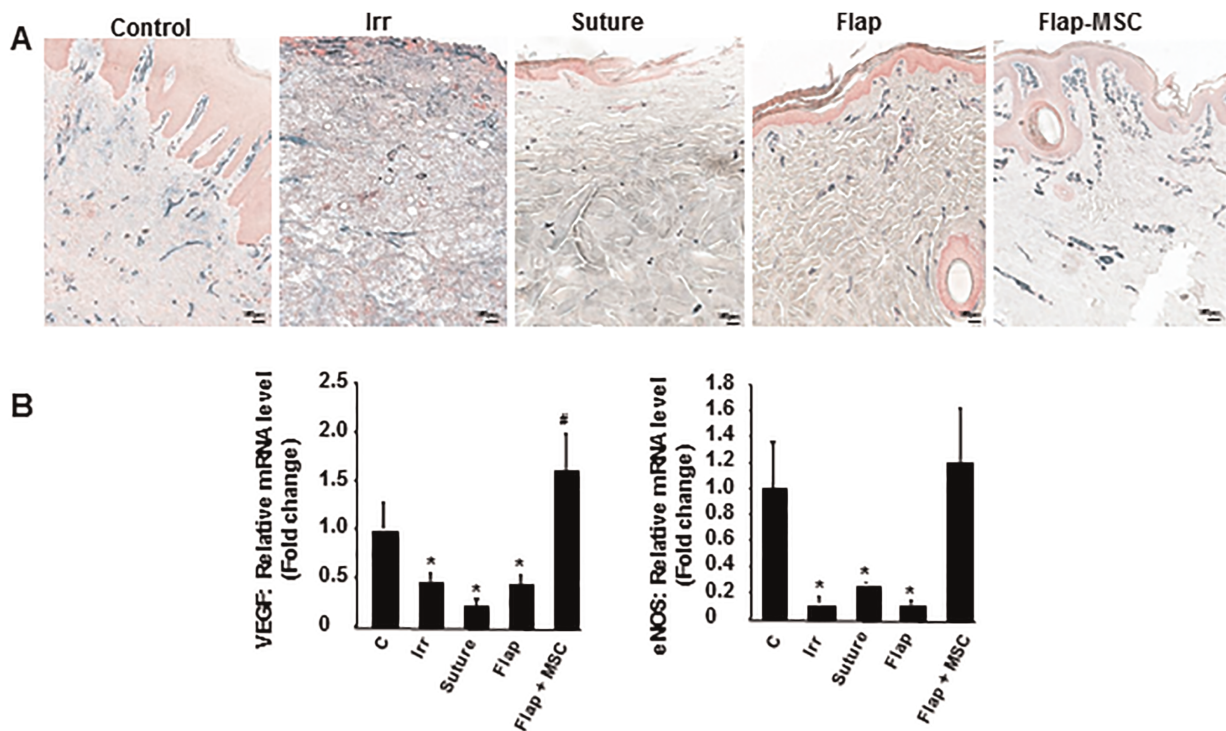
Figure 7. MSC injections accelerated and stabilized vascular restoration after flap surgery. **(A):** Representative immunostaining of Van Willebrand factor. **(B):** Real-time expression of angiogenic factors VEGF and eNOS. Scale bar: 150 μm. Results are expressed as means ± SEM. p values were calculated by ANOVA with Bonferroni correction, *, $p < .05$ compared with nonirradiated controls; #, $p < .05$ compared with irradiated controls. Abbreviations: eNOS, endothelial nitric oxide synthase; MSC, mesenchymal stromal cell; VEGF, vascular endothelial growth factor.

the deep dermis, indicative of marked remodeling. A year after both suture and flap surgery, however, the TUNEL-positive cells remained higher than in the nonirradiated skin, albeit lower than in the irradiated skin, while their level in the flap-MSC skin was similar to that in the nonirradiated skin. The apoptotic cells quantification confirmed the normalization of the TUNEL staining observed with the BM-MSC treatment (Fig. 6F).

MSC Injections Accelerated Restoration of Vascular Structures

Numerous studies have demonstrated the proangiogenic role of MSCs [28], but the long-term maintenance of the vascular structure has remained unknown. We used immunohistochemical labeling for Van Willebrand factor to observe the blood vessels. Irradiated skin showed a paucity of blood vessels compared with nonirradiated skin (Fig. 7A). A year after surgery the number of vascular structures remained limited in the suture and flap groups and were found mainly in the papillary dermis. In contrast, the flap-MSC skin contained significantly more vascular structures, with the vessels taking on a vertically oriented pattern perpendicular to the skin surface, similar to the structure of nonirradiated skin. The loss of vessels observed the day of surgery and a year later in the suture and flap groups was confirmed by the repression of angiogenic factors such as VEGF and eNos, compared with their levels in nonirradiated skin (Fig. 7B). In the flap-MSC skin, vessel restoration was accompanied by the normalization of VEGF and eNos expression.

DISCUSSION

Current research on irradiation burns is focusing on the regeneration of functional skin with integrity similar to that of the intact tissue surrounding it. Long-term medical attention is generally needed, with a period of at least 6–18 months required for the maturation of thermal burn scars [10]. The difficulty in treating cutaneous radiation syndrome lies in the unpredictable inflammatory waves that can recur weeks to years after tissue injury: they make healing fragile and unstable over time and conventional surgical treatment ineffective [2]. It now appears that stem cell therapy combined with surgery may become indispensable for treatment of high-grade radiation injuries. The aim of this study was to assess the quality of long-term wound healing after conventional resection of necrotic tissue and the placement of a vascularized flap and, especially, the added benefits of MSC therapy, expanded according to a clinical-grade protocol and associated with the flap surgery.

The remodeling/resolution phase of wound healing, in contrast to the much shorter phases preceding, it (hemostasis and proliferation) can last for months to years and is thought to be delayed in skin-related fibrotic disorders such as keloid scarring. The risk of impaired wound healing is particularly important with irradiated skin, where the unpredictable spatiotemporal course of inflammatory waves [1] increases the incidence of fibrosis. Our data confirmed that the remodeling process fails after simple resection of fibrotic-necrotic tissue and results in the long term in a hypertrophic scar. Clinical observations in this study showed that the scars in the group receiving

Long term wound healing of irradiated tissue

Suture	Flap	Flap-MSC
Fibrotic matrix	Immature matrix	Mature matrix
↓	↓	↓
Matrikines, MMPs generate signals to recruit inflammatory cells	Matrikines, MMPs generate signals to recruit inflammatory cells	Balanced collagen
↓	↓	↓
Fibroblast hyperproliferation Myofibroblast persistence Collagen imbalance Collagen1 domination	More Immature matrix generation Collagen imbalance Collagen 3 domination	Maintenance of vessels
↓	↓	↓
Excess ECM production	Fibroblast activation Matrix contraction / Tension	Fibroplasia suppression
↓	↓	↓
Hypertrophic scar	Cell death/ Vessel loss	Wound healing with minimal scarring
	↓	
	Failure of resolution Chronic wound	

Figure 8. Schematic diagram of wound healing of irradiated skin, according to treatment. The resection of fibrotic areas restarts fibroblastic activation and drives excess ECM production that produces a hypertrophic scar. Vascularized flap surgery generates an immature ECM, due to defective ECM protein production, and causes the persistence of inflammatory nodules and vessel loss. MSC therapy associated with the vascularized flap surgery provided durable repair by stabilizing fibroblast activation, thus helping to produce a mature ECM devoid of inflammation and leading to vascular stability. Abbreviations: ECM, extracellular matrix; MMP, matrix metalloproteinase; MSC, mesenchymal stromal cell.

simple suture surgery to cover cutaneous defects appeared hypertrophic at 8 months after surgery and were retractile at 12 months. On the contrary, the scars in both flap surgery groups (with and without MSC treatment) were visually nonpathologic.

Optimal outcome of cutaneous wound healing involves regeneration of the normal architecture and function of the skin. Histological analysis showed that BM-MSC treatment re-established both epithelization limiting epidermal atrophy induced by irradiation and dermal thickness. Probably, BM-MSCs acted on epithelization by enhancing proliferation of resident epidermal cells in the presence of epidermal growth factor, possibly produced by bone marrow cells or by their differentiation into epidermal cells [29]. In the dermal level collagens control tissue architecture, tensile strength, and cell-ECM interaction, and organized collagen deposition is associated with improved wound maturation. Among the characteristic histological changes in irradiated skin, a unilateral arrangement of collagen fibers has been previously reported in patients with complications after expander/implant reconstruction of irradiated skin [30]. We thus noted that the multidirectional arrangement of collagen was not restored in the long term after simple excision of the fibrotic/necrotic area, but was re-established after flap surgery (with and without MSC treatment).

Interstitial collagens type 1 and type 3 are major constituents of the ECM that supports skin structure. Although type 1 and type 3 collagen fibers coexist within individual fibrils, their relative ratios play an important role in the regulation of fibrillogenesis and in the determination of the final fibular diameter and bundle architecture [31], with the mature type-1 collagen responsible for mechanical stability, whereas type-3 collagen forms thin fibers and can be regarded as immature collagen of the early wound healing process. In our study, immunohistologic and gene expression analyses revealed a predominance of collagen deposition with excess levels of

Col1 in the suture surgery group and Col3 in the flap group. This collagen imbalance may signal the failure to transition to the resolution phase. Col1 excess is an indicator of pathological scarring evolving to fibrosis [32]. Likewise, and compared with nonirradiated skin, the higher proportion of Col3 relative to Col1, combined with the increased fiber thickness observed in the flap, may be related to either immature wound healing or a chronic wound [33]. Our study shows that MSC injections normalized both Col3 and 1 deposition.

Moreover, collagen degradation is as important as collagen synthesis in the process of wound healing. It involves MMPs and TIMPs [12]. The collagen-to-MMP-to-TIMP ratios in our study confirm elevated collagen production in both the suture and simple flap surgery groups, resulting in the failure of the matrix to mature. When flap surgery was combined with MSC treatment, however, the balance of collagen synthesis/degradation was restored and, especially, maintained over the long term.

ECM composition and organization are controlled by ECM proteins such as decorin and fibronectin. These proteins, which are reported to prevent fibrosis [34], have been shown to be expressed at similar levels in mature scars and in normal skin. These levels, however, are reduced in early wound healing and delayed in abnormal wound healing (such as in post-irradiation hypertrophic scars) [22]. Consistent with this pathophysiological range, immunostaining and gene expression revealed that after flap surgery and MSC treatment both decorin and fibronectin levels were similar to those of normal skin, while their expression was insufficient after both suture surgery and flap surgery alone. Inflammation clearly influences the wound repair process [24]. In the immature matrix, downregulation of decorin and fibronectin, associated with chronic inflammation, induced continued matrix production, and a lack of tissue architecture. This damage is particularly drastic when inflammation occurs late, during the regenerative and resolving phases. In irradiation contexts, little is known about how inflammation reappears during a late phase, long after

exposure: what stimulus incites it? What signal failures cause the inflammatory response to continue? In the group with suture surgery and even in the group with a vascularized flap (but no MSCs), notable macrophage staining persisted a year after surgery and was seen as an inflammatory nodule in both the papillary and the deep dermis.

In this study, we used the Mac387 antibody, because it recognizes calprotectin, which is associated with the cytoskeleton of neutrophils, monocytes, and a subset of reactive macrophages during the early stage of monocyte/macrophage differentiation. Interestingly, excess calprotectin over a long period appears to cause local tissue destruction, including by inducing apoptosis in fibroblasts [35]. Inversely, the macrophages were also responsible for clearing apoptotic cells, thus impelling resolution of the inflammation. Macrophages thus appear to promote transition to the proliferative phase of healing. Figure 6E, at the same time that it depicts the increase of Mac387-positive cell staining, shows the strong presence of apoptotic cells in the irradiated skin and their continuing importance in both the suture and flap surgery groups. At this point in time (1 year after surgery), it remained difficult to differentiate chronic wound inflammation from delayed/unfinished wound healing occurring in the flap surgery. On the contrary, in the group with flap surgery and MSC treatment, the levels of both apoptotic cells and Mac387-positive cells were similar to those in normal skin.

Until now, the long-term persistence of the anti-inflammatory process induced by the MSC injection was unknown. Some reports showed that fibroblasts were the cell type mainly responsible for both synthesizing and degrading ECM components. Of interest for scarring, these studies also showed that both collagen fragments released during degradation and endogenous molecules released from necrotic tissue are chemotactic for inflammatory cells [36]. In this study, we observed the fibroblast presence as a nodule, displayed by S100a4 staining, in the flap surgery group, whereas with the MSC treatment fibroblast distribution was homogenous throughout the deep dermis. The persistence of fibroblast activation areas contributed to the imbalance in the ECM synthesis/degradation process [26]; MSC treatment, by stabilizing fibroblast activation, might compromise the positive feedback loop between excessive ECM protein in dermal fibroblasts and inflammation.

The achievement of durable wound healing requires the formation of a vascular network to regenerate the wound. Imbalanced angiogenesis regulation can result in abnormal scarring, delayed wound healing, and chronic wound formation. Many ECM molecules, including collagen and fibronectin, have proangiogenic properties that promote endothelial cell survival (which depends on cell–ECM interactions), growth, migration, and tube formation [37]. By sequestering angiogenic factors, the ECM plays an important role in stabilizing blood vessels, which is particularly essential in the remodeling phase [37]. Endothelial cell differentiation/migration and tube formation all occur in the absence of fibronectin, but the maintenance of the vessel requires fibronectin. This maintenance state is especially important in the late phase of remodeling. We noted in this study that ECM quality was similar in flap-MSC skin and nonirradiated skin and associated with similar levels of vascular density and angiogenic factors (VEGF, eNOS). Interestingly, fibronectin bound to VEGF and enhanced VEGF-induced endothelial cell migration [38].

CONCLUSION

In the cutaneous radiation syndrome, ECM synthesis is an important step in the skin regeneration process, resulting in tissue remodeling with less scar formation and long-term maintenance of wound healing with neither inflammation nor recurrent fibrosis. On irradiated tissue, simple excision of fibrotic areas reinitiates fibroblastic activation that drives excess ECM production and results in a hypertrophic scar (Fig. 8). Vascularized flap surgery appears to prevent excessive ECM deposition; but the failure to produce ECM proteins prevents the matrix from maturing over the long term, resulting in persistence of inflammatory nodules and loss of vessels. The MSC therapy associated with vascularized flap surgery provided durable repair, probably by stabilizing fibroblast activation and ECM protein expression, therefore contributing to a mature ECM devoid of inflammation and enabling vascular stability.

AUTHOR CONTRIBUTIONS

C.L.: conception and design, collection and data analysis and interpretation, manuscript writing, final approval of manuscript; M.B.: animal surgery, conception and design, collection and data analysis and interpretation, manuscript writing, critical revision, final approval of manuscript; E.B.: animal surgery, conception and design, critical revision, final approval of manuscript; C.S., B.L., and M.B.: animal assistance and technical support; E.B.: cell technical issue; C.S. and V.H.: technical support; J.-J.L. and M.B.: conception and design, critical revision of the manuscript, final approval of manuscript.

DISCLOSURE OF POTENTIAL CONFLICTS OF INTEREST

The authors indicated no potential conflicts of interest.

REFERENCES

1 Zhao W, Robbins ME. Inflammation and chronic oxidative stress in radiation-induced late normal tissue injury: Therapeutic implications. Curr Med Chem 2009;16:130–143.

2 Bey E, Prat M, Duhamel P et al. Emerging therapy for improving wound repair of severe radiation burns using local bone marrow-derived stem cell administrations. Wound Repair Regen 2010;18:50–58.

3 Wu Y, Wang J, Scott PG et al. Bone marrow-derived stem cells in wound healing: A review. Wound Repair Regen 2007;15:S18–S26.

4 Lataillade JJ, Doucet C, Bey E et al. New approach to radiation burn treatment by dosimetry-guided surgery combined with autologous mesenchymal stem cell therapy. Regen Med 2007;2:785–794.

5 François S, Mouiseddine M, Mathieu N et al. Human mesenchymal stem cells favour healing of the cutaneous radiation syndrome in a xenogenic transplant model. Ann Hematol 2006;86:1–8.

6 Agay D, Scherthan H, Forcheron F et al. Multipotent mesenchymal stem cell grafting to treat cutaneous radiation syndrome: Development of a new minipig model. Exp Hematol 2010;38:945–956.

7 Leclerc T, Thepenier C, Jault P et al. Cell therapy of burns. Cell Prolif 2011;44:48–54.

8 Horton JA, Hudak KE, Chung EJ et al. Mesenchymal stem cells inhibit cutaneous radiation-induced fibrosis by suppressing chronic inflammation. Stem Cells 2013;31: 2231–2241.

9 McFarlin K, Gao X, Liu YB et al. Bone marrow-derived mesenchymal stromal cells accelerate wound healing in the rat. Wound Repair Regen 2006;14:471–478.

10 Gauglitz GG, Korting HC, Pavicic T et al. Hypertrophic scarring and keloids: Pathomechanisms and current and emerging treatment strategies. Mol Med 2011;17: 113–125.

11 Gurtner GC, Werner S, Barrandon Y et al. Wound repair and regeneration. Nature 2008;453:314–321.

12 Linard C, Tissedre F, Busson E et al. Therapeutic potential of gingival fibroblasts for cutaneous radiation syndrome: Comparison to bone marrow-mesenchymal stem cell grafts. Stem Cells Dev 2015;24: 1182–1193.

13 Benderitter M, Gourmelon P, Bey E et al. New emerging concepts in the medical management of local radiation injury. Health Phys 2010;98:851–857.

14 Zhang J, Huang X, Wang H et al. The challenges and promises of allogeneic mesenchymal stem cells for use as a cell-based therapy. Stem Cell Res Ther 2015;6:234.

15 Swindle MM, Makin A, Herron AJ et al. Swine as models in biomedical research and toxicology testing. Vet Pathol 2012;49: 344–356.

16 Linard C, Busson E, Holler V et al. Repeated autologous bone marrow-derived mesenchymal stem cell injections improve radiation-induced proctitis in pigs. Stem Cells Translational Medicine 2013;2: 916–927.

17 Brink N, Szamel M, Young AR et al. Comparative quantification of IL-1beta, IL-10, IL-10r, TNFalpha and IL-7 mRNA levels in UV-irradiated human skin in vivo. Inflamm Res 2000;49:290–296.

18 Nagai N, Hosokawa M, Itohara S et al. Embryonic lethality of molecular chaperone hsp47 knockout mice is associated with defects in collagen biosynthesis. J Cell Biol 2000;150:1499–1506.

19 Dafforn TR, Della M, Miller AD. The molecular interactions of heat shock protein 47 (Hsp47) and their implications for collagen biosynthesis. J Biol Chem 2001;276:49310–49319.

20 Hadler-Olsen E, Fadnes B, Sylte I et al. Regulation of matrix metalloproteinase activity in health and disease. FEBS J 2011; 278:28–45.

21 Sandler NG, Mentink-Kane MM, Cheever AW et al. Global gene expression profiles during acute pathogen-induced pulmonary inflammation reveal divergent roles for Th1 and Th2 responses in tissue repair. J Immunol 2003;171:3655–3667.

22 Sayani K, Dodd CM, Nedelec B et al. Delayed appearance of decorin in healing burn scars. Histopathology 2000;36: 262–272.

23 Darby IA, Laverdet B, Bonté F et al. Fibroblasts and myofibroblasts in wound healing. Clin Cosmet Investig Dermatol 2014;7:301–311.

24 Stramer BM, Mori R, Martin P. The inflammation–fibrosis link? A Jekyll and Hyde role for blood cells during wound repair. J Invest Dermatol 2007;127:1009–1017.

25 Wu Y, Huang S, Enhe J et al. Bone marrow-derived mesenchymal stem cell attenuates skin fibrosis development in mice. Int Wound J 2014;11:701–710.

26 Yates CC, Bodnar R, Wells A. Matrix control of scarring. Cell Mol Life Sci 2011;68: 1871–1881.

27 Wells A, Nuschke A, Yates CC. Skin tissue repair: Matrix microenvironmental influences. Matrix Biol 2016;49:25–36.

28 Maranda EL, Rodriguez-Menocal L, Badiavas EV. Role of mesenchymal stem cells in dermal repair in burns and diabetic wounds. Curr Stem Cell Res Ther 2017;12: 61–70.

29 Kataoka K, Medina RJ, Kageyama T et al. Participation of adult mouse bone marrow cells in reconstitution of skin. Am J Pathol 2003;163:1227–1231.

30 Iwahira Y, Nagase T, Nakagami G et al. Histopathological comparisons of irradiated and non-irradiated breast skin from the same individuals. J Plast Reconstr Aesthet Surg 2012;65:1496–1505.

31 Si Z, Bhardwaj R, Rosch R et al. Impaired balance of type I and type III procollagen mRNA in cultured fibroblasts of patients with incisional hernia. Surgery 2002; 131:324–331.

32 Friedman DW, Boyd CD, Mackenzie JW et al. Regulation of collagen gene expression in keloids and hypertrophic scars. J Surg Res 1993;55:214–222.

33 Klinge U, Si ZY, Zheng H et al. Collagen I/III and matrix metalloproteinases (MMP) 1 and 13 in the fascia of patients with incisional hernias. J Invest Surg 2001;14:47–54.

34 Honardoust D, Varkey M, Hori K et al. Small leucine-rich proteoglycans, decorin and fibromodulin, are reduced in post-burn hypertrophic scar. Wound Repair Regen 2011;19:368–378.

35 Yui S, Nakatani Y, Mikami M. Calprotectin (S100A8/S100A9), an inflammatory protein complex from neutrophils with broad apoptosis-inducing activity. Biol Pharm Bull 2003;26:753–760.

36 Sorokin L. The impact of the extracellular matrix on inflammation. Nat Rev Immunol 2010;10:712–723.

37 Sottile J. Regulation of angiogenesis by extracellular matrix. Biochim Biophys Acta 2004;1654:13–22.

38 Wijelath ES, Murray J, Rahman S et al. Novel vascular endothelial growth factor binding domains of fibronectin enhance vascular endothelial growth factor biological activity. Circ Res 2002;91:25–31.

See www.StemCellsTM.com for supporting information available online.